Hindawi Publishing Corporation
Journal of Nanomaterials
Volume 2014, Article ID 769618, 7 pages
http://dx.doi.org/10.1155/2014/769618

Research Article

Effects of Wavenumber and Chirality on the Axial Compressive Behavior of Wavy Carbon Nanotubes: A Molecular Mechanics Study

Masaki Kawachi,[1] Yusuke Kinoshita,[1,2] and Nobutada Ohno[1,2]

[1] *Department of Computational Science and Engineering, Nagoya University, Furo-cho, Chikusa-ku, Nagoya 464-8603, Japan*
[2] *Department of Mechanical Science and Engineering, Nagoya University, Furo-cho, Chikusa-ku, Nagoya 464-8603, Japan*

Correspondence should be addressed to Masaki Kawachi; kawachi@mml.mech.nagoya-u.ac.jp

Received 24 June 2014; Revised 16 September 2014; Accepted 16 September 2014; Published 13 October 2014

Academic Editor: Chunyi Zhi

The effects of wavenumber and chirality on the axial compressive behavior and properties of wavy carbon nanotubes (CNTs) with multiple Stone-Wales defects are investigated using molecular mechanics simulations with the adaptive intermolecular reactive empirical bond-order potential. The wavy CNTs are assumed to be point-symmetric with respect to their axial centers. It is found that the wavy CNT models, respectively, exhibit a buckling point and long wavelength buckling mode regardless of the wavenumbers and chiralities examined. It is also found that the wavy CNTs have nearly the same buckling stresses as their pristine straight counterparts.

1. Introduction

Carbon nanotubes (CNTs) have a higher specific strength than conventional materials; for example, the density and Young's modulus of steels are about 8 g/cm^3 and 200 GPa, respectively, whereas those of CNTs are 2 g/cm^3 and 1 TPa [1–3]. Thus, CNTs are expected to be a constituent of composite materials, nanoprobe, and micro/nanoelectromechanical systems (MEMS/NEMS). To avoid mechanical failure and the breaking of structures including CNTs, it is important to obtain not only the tensile properties, but also the compressive properties of CNTs. However, there have been very few experimental tests to obtain the axial compressive properties of CNTs [4, 5] because it is difficult to conduct axial compressive experiments of CNTs with small diameters and high aspect ratios.

Using atomistic simulations rather than experimental tests, many researchers have analyzed the axial compressive properties of CNTs [6–13]. For example, Sears and Batra analyzed the axial buckling behaviors of pristine, single-walled (SW), and multiwalled (MW) CNTs [6, 7]. Xin et al. studied the axial compressive properties of SWCNTs with vacancies and reported that their compressive strength shows temperature independence [8]. It is noteworthy that the CNTs analyzed by these researchers have defects at only one site along the tube axial direction [6–13]. On the other hand, actual CNTs observed through experiments (Figure 1) have defects at multiple sites, resulting in a wavy geometry or multiple bending [4, 5].

The authors analyzed the axial compressive buckling behaviors of wavy SWCNTs with different waveforms, wavelengths, amplitudes, and tube lengths using molecular mechanics (MM) simulations [14]. In the simulations, because CNTs are usually bent inherently by Stone-Wales (SW) defects [15, 16], wavy CNTs were modeled by inserting multiple SW defects at different heights of a tube, resulting in the following findings under axial compression. C-shaped, point-asymmetric wavy CNTs with respect to their tube axial centers did not show any buckling point, and their axial compressive stresses asymptotically approached the axial compressive stress-strain curves of their pristine straight counterparts. In contrast, S-shaped, point-symmetric wavy CNTs, respectively, exhibited a buckling point and had nearly the same buckling stresses as their pristine straight counterparts. This was because *long wavelength compressive buckling*

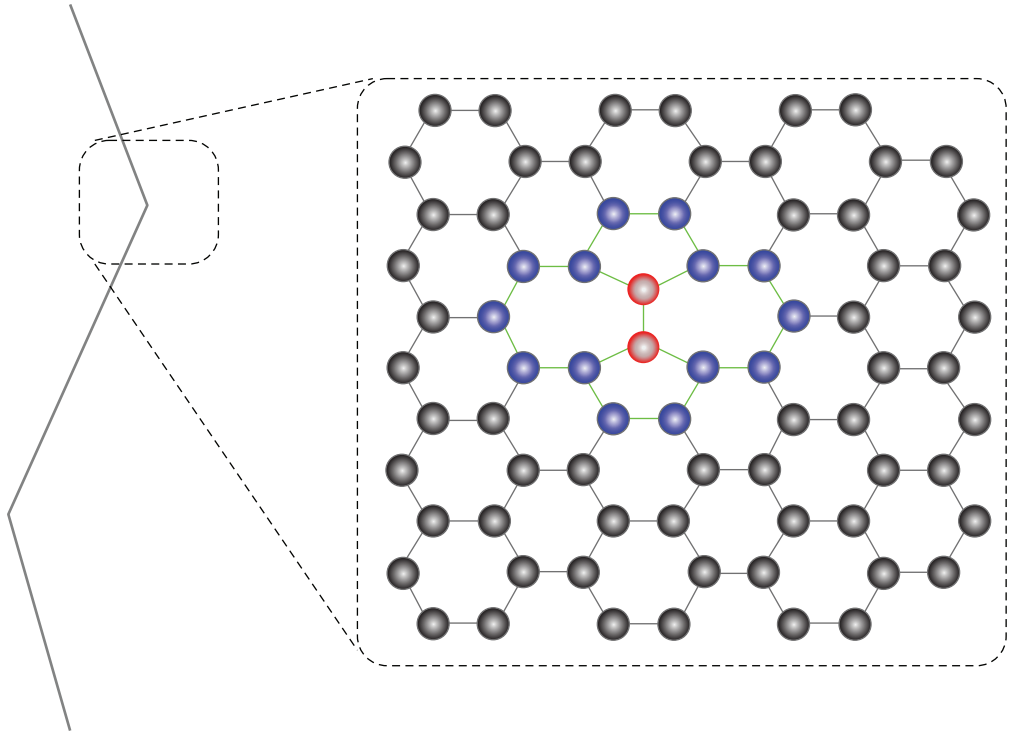

Figure 1: Schematics of part of an experimentally observed CNT, which has multiple SW defects.

occurred despite the S-shaped, initial geometrical imperfection; in other words, axial compressive buckling dominated the instability of S-shaped CNTs under axial compression in the same way as that of straight CNTs. The simulations by the authors also showed that the axial compressive strengths of C- and S-shaped wavy CNTs hardly depended on their waveforms, wavelengths, and amplitudes and were predicted well by the Euler buckling theory using Young's modulus of 1 TPa.

Remaining issues are the effects of wavenumber and chirality of wavy CNTs on their axial compressive buckling behavior. In the previous paper [14], wavenumber and chiral index of wavy CNTs were one and (6, 0), respectively, whereas actual CNTs have various wavenumbers and chiralities. Thus, in this study, the effects of wavenumber and chirality on the axial compressive buckling behavior of S-shaped point-symmetric wavy SWCNTs with multiple SW defects are evaluated using MM simulations with the adaptive intermolecular reactive empirical bond-order (AIREBO) potential [17].

2. Simulation Procedure

2.1. Models. Figure 2 shows the schematics and snapshots of the simulation models. The Zigzag_wavy1 model has six SW defects, point-symmetric geometry, one wavenumber, and a (6, 0) chiral index. The bent angle α is about 7° at the positions of the SW defects. With reference to the Zigzag_wavy1 model, we prepared the Zigzag_wavy2 model with two wavenumbers in order to investigate the effects of wavenumber on the axial compressive buckling behavior of wavy CNTs. To analyze the effects of chirality, we prepared (4, 4) wavy SWCNTs with one and two wavenumbers, the Armchair_wavy1 and Armchair_wavy2 models. These models have nearly the same length L, diameter D, and amplitude A as the Zigzag_wavy1 and Zigzag_wavy2 models (Table 1). Pristine straight counterparts (Zigzag_straight, Armchair_straight) were also analyzed for comparison. The distance between nearest neighboring atoms a and the tube thickness t are 0.142 and 0.335 nm, respectively. The diameter D of a tube with (m, n) chiral index is calculated by the following equation:

$$D = \frac{\sqrt{3}a}{\pi}\sqrt{m^2 + mn + n^2}. \quad (1)$$

2.2. Molecular Mechanics. In this study, compressive analyses were conducted using MM simulations with AIREBO potential [17]. Load-free stable configurations of the simulation models were initially obtained using the FIRE algorithm [18], so that the axial stress σ and atomic forces dropped below 0.01 GPa and 1.6 fN, respectively. Then, the axial compressive strain ε was applied to the models by incrementally displacing the top end atoms in the negative axial direction while the bottom end atoms were fixed. Compressive forces were thus induced among the atoms in CNTs. In this study, ε was in the range from 0 to 0.02 with an increment $\Delta\varepsilon$ of 0.0005. After each increment of strain, the atomic configurations were relaxed using the FIRE algorithm until each atomic force decreased below 1.6 fN.

In parallel with the axial compressive analysis, an instability analysis [19, 20] was performed in order to judge the buckling point and detect the buckling mode of wavy CNTs. In atomic instability analysis, the stability or instability of

Table 1: Equilibrium length L, diameter D, and amplitude A of the simulation models.

Model	L (nm)	D (nm)	A (nm)	L/D	L/A
Zigzag_straight	19.809	0.470	—	42.1	—
Zigzag_wavy1	19.712	0.470	0.100	41.9	197.1
Zigzag_wavy2	19.616	0.470	0.097	41.7	202.2
Armchair_straight	21.309	0.542	—	39.3	—
Armchair_wavy1	21.406	0.542	0.112	39.5	191.1
Armchair_wavy2	21.503	0.542	0.112	39.7	192.0

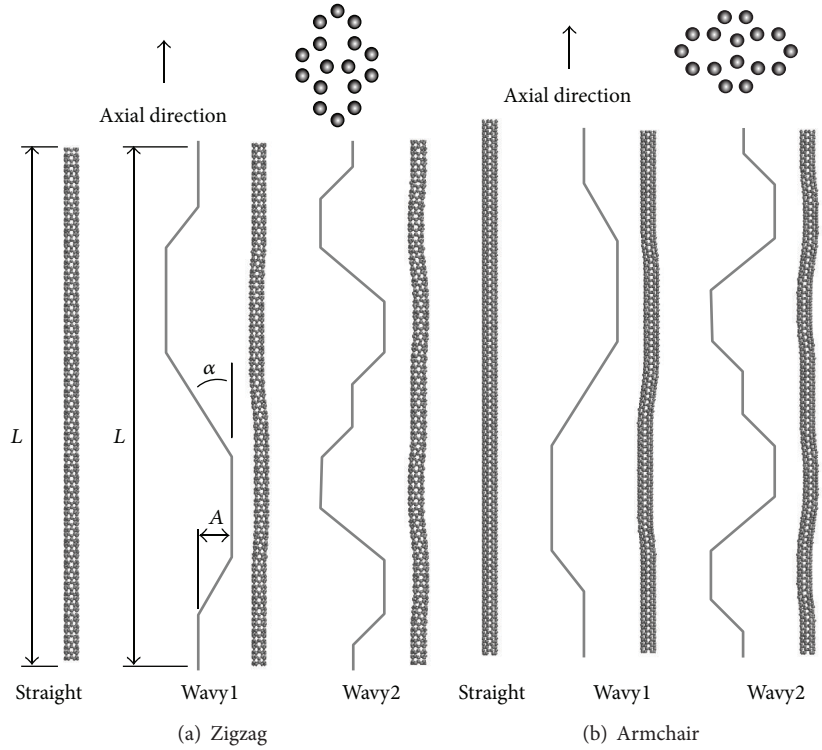

Figure 2: Schematics and snapshots of the simulation models.

an atomic system was determined by the positivity of the Hessian matrix **H** of the potential energy with respect to the atomic coordinates. The eigenvalues of **H** represent the principal curvature of the energy surface of an atomic system with respect to arbitrary infinitesimal atomic position changes. An atomic system is stable when the minimum eigenvalue of **H** is positive and becomes unstable when the minimum eigenvalue of **H** reaches 0. In this analysis, the buckling point of a wavy CNT was defined as the point at which the minimum eigenvalue was 0, and the buckling mode was detected as the eigenvector corresponding to the minimum eigenvalue.

3. Results and Discussion

Figure 3(a) shows the compressive stress-strain curves of the Zigzag_wavy1 (blue dashed line) and the Zigzag_wavy2 (green line) models [21]. In the figure, a black dot indicates a buckling point. Both of the stress-strain curves consist of three phases. Firstly, before buckling, the compressive stress of the Zigzag_wavy1 and Zigzag_wavy2 models increases linearly with the compressive strain. Secondly, at the buckling point, both the models exhibit nearly the same buckling stresses of about 3.3 GPa. Thirdly, after buckling, these compressive stresses plateau. In other words, both the wavy models exhibit nearly the same compressive stress-strain relationship. The only noteworthy feature is that the Zigzag_wavy1 and Zigzag_wavy2 models differ in the wavenumber; the other geometrical features are nearly the same. Thus, the compressive stress-strain relationship of wavy CNTs hardly depends on wavenumber.

Figure 3(b) shows the compressive stress-strain curves of the Zigzag_wavy1 and the Armchair_wavy1 (red line) models. The stress-strain curve of the Armchair_wavy1 model also consists of three phases: linear increase of the compressive stress before buckling, a buckling point of 3.3 GPa, and

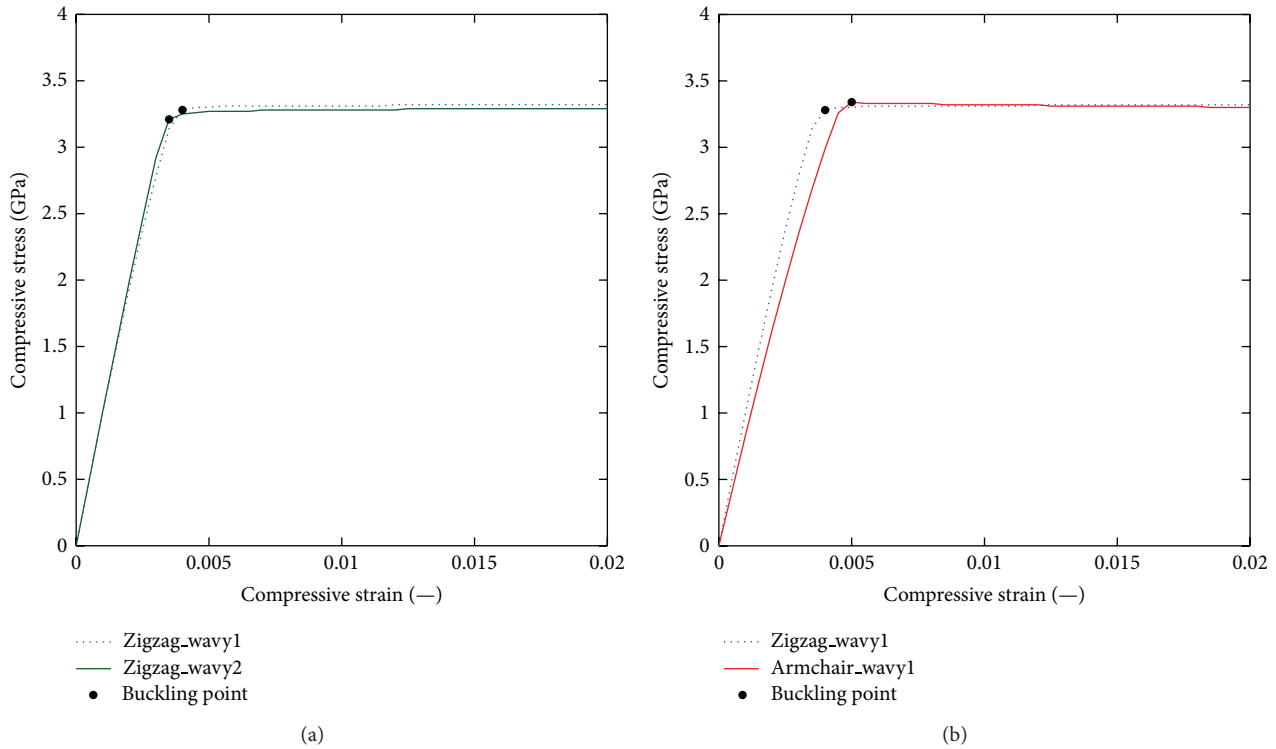

Figure 3: Compressive stress-strain curves of (a) Zigzag_wavy2 and (b) Armchair_wavy1 models with reference to the Zigzag_wavy1 model.

a plateau after buckling. As mentioned in Section 2.1, the Armchair_wavy1 and the Zigzag_wavy1 models have nearly the same geometries, except for their chirality. Thus, the compressive stress-strain relationship of wavy CNTs hardly depends on chirality.

Table 2 lists the buckling stress of all the simulation models. The wavy CNT models exhibit a buckling point regardless of their wavenumber or chirality and show nearly the same buckling stresses as their pristine straight counterparts. Therefore, these results indicate that the buckling stress of wavy CNTs hardly depends on wavenumber or chirality.

Figure 4 shows snapshots of the Zigzag_wavy1, Zigzag_wavy2, and Zigzag_straight models before compression ($\varepsilon = 0$), at buckling point ($\varepsilon = \varepsilon_c$), and after buckling ($\varepsilon = 0.02$). Before buckling, the amplitudes of the Zigzag_wavy1 and Zigzag_wavy2 models increase while keeping their point-symmetric waveform, and the Zigzag_straight model retains a straight shape. After buckling, all of the models changed into point-asymmetric C-shapes with longer wavelengths than their initial shapes. The deformation behavior of the Armchair models is similar to that of the Zigzag models (Figure 5). Therefore, the buckling deformation behavior of wavy CNTs hardly depends on wavenumber or chirality.

In order to clarify the reason that wavy CNTs exhibit the same buckling behavior regardless of their wavenumber or chirality, an instability analysis [19, 20] was performed. Figure 6 shows the eigenvalues corresponding to the first (C-shaped), the second (S-shaped), and the fourth (initial waveform) eigenmodes of the Zigzag_wavy2 model as a function of the axial compressive strain. The inset in the figure schematically illustrates the first, second, and fourth eigenmodes of the Zigzag_wavy2 model. As mentioned in Section 2.2, when the minimum eigenvalue $\eta_{\min}$ reaches zero in the compressive process, an atomic system becomes unstable in the eigenmode corresponding to $\eta_{\min}$. As shown in Figure 6, the minimum eigenvalue $\eta_{\min}$ (first mode) reaches zero at the buckling point in Figure 3. The eigenmode corresponding to $\eta_{\min}$ is a long wavelength (C-shaped) buckling mode, which is consistent with the actual deformation shape (Figure 4(c)). On the other hand, the eigenvalues corresponding to the S-shaped and initial waveform eigenmodes do not reach zero. These results are also true for the other wavy models. Therefore, the wavy CNTs deform under the long wavelength (C-shaped) buckling mode, regardless of their wavenumber or chirality.

Table 2: Buckling stress of the simulation models.

Model	Buckling stress (GPa)
Zigzag_straight	3.32
Zigzag_wavy1	3.30
Zigzag_wavy2	3.21
Armchair_straight	3.52
Armchair_wavy1	3.34
Armchair_wavy2	3.10

The results in this paper have also demonstrated that atomic systems are able to exhibit long wavelength buckling. In continuum solid mechanics, it has already been clarified

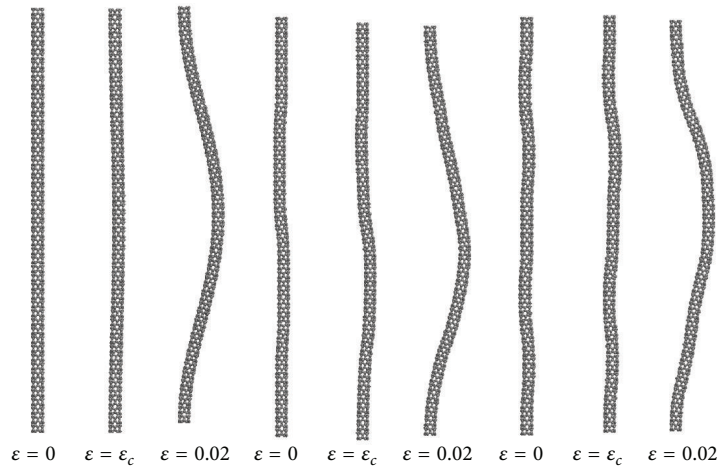

Figure 4: Snapshots of the Zigzag models during axial compression.

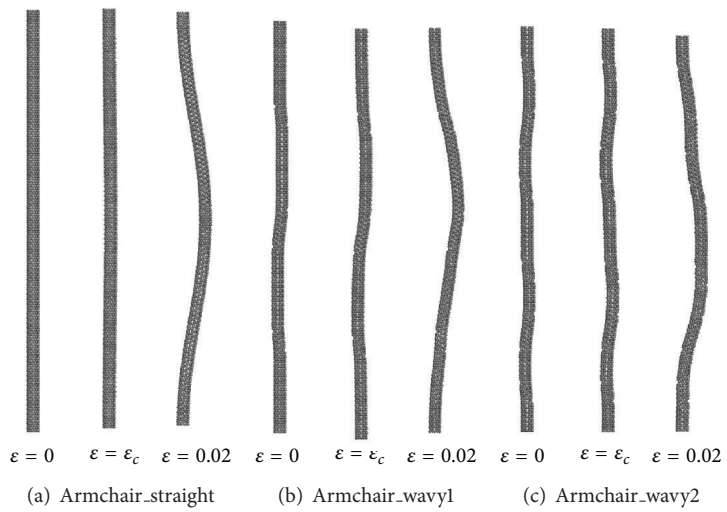

Figure 5: Snapshots of the Armchair models during axial compression.

that periodic solids are able to bifurcate into long wavelength buckling modes [22, 23]. If the wavy CNTs analyzed in this study could be modeled as continuum thin walled tubes with appropriate material parameters, it might be shown that such continuum models also reproduce the long wavelength buckling behavior revealed in this paper. However, this is an issue in the future because continuum modeling of SW defects is open to discussion [24].

4. Conclusions

In this study, the effects of wavenumber and chirality on the axial compressive buckling behavior of wavy CNTs with multiple SW defects have been studied using MM simulations with the AIREBO potential. The wavy CNTs have been assumed to be point-symmetric with respect to their axial centers. The key findings are that the wavy CNT models, respectively, exhibit a buckling point and have nearly the same buckling stresses as their pristine straight counterparts, regardless of the wavenumbers and chiralities examined. In other words, the buckling stress of wavy CNTs depends on the tube length but hardly on the wavenumber and chirality.

The results in this paper have also demonstrated that atomic systems are able to exhibit long wavelength buckling. In continuum solid mechanics, it has already been clarified that periodic solids are able to bifurcate into long wavelength buckling modes [22, 23]. If the wavy CNTs analyzed in this study could be modeled as continuum thin walled tubes with appropriate material parameters, it might be shown that such continuum models exhibit long wavelength buckling similar to MM simulation models. However, this is an issue in the

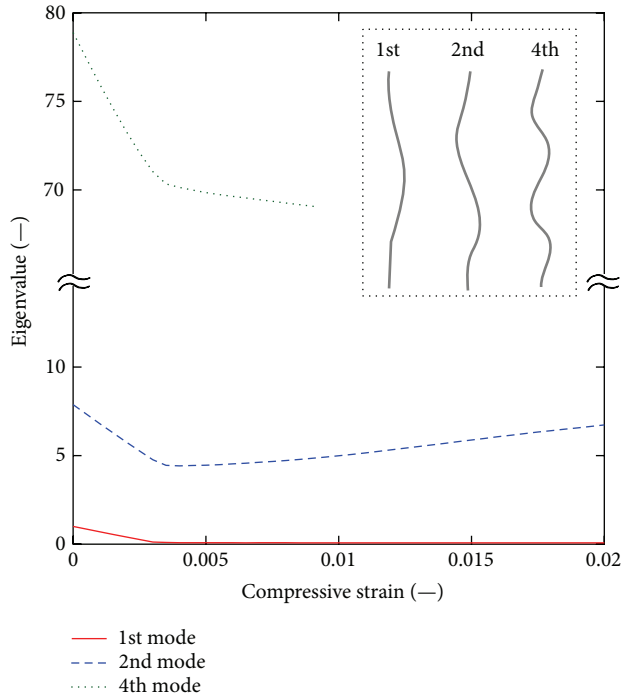

Figure 6: Eigenvalues corresponding to the first (C-shaped), the second (S-shaped), and the fourth (initial waveform) eigenmodes of Zigzag_wavy2 model as a function of the axial compressive strain; the inserted figure schematically illustrates the first, second, and fourth eigenmodes of the Zigzag_wavy2 model.

future because continuum modeling of SW defects is open to discussion [24].

Conflict of Interests

The authors declare that there is no conflict of interests regarding the publication of this paper.

References

[1] M. M. J. Treacy, T. W. Ebbesen, and J. M. Gibson, "Exceptionally high Young's modulus observed for individual carbon nanotubes," *Nature*, vol. 381, no. 6584, pp. 678–680, 1996.

[2] M.-F. Yu, O. Lourie, M. J. Dyer, K. Moloni, T. F. Kelly, and R. S. Ruoff, "Strength and breaking mechanism of multiwalled carbon nanotubes under tensile load," *Science*, vol. 287, no. 5453, pp. 637–640, 2000.

[3] B. Peng, M. Locascio, P. Zapol et al., "Measurements of near-ultimate strength for multiwalled carbon nanotubes and irradiation-induced crosslinking improvements," *Nature Nanotechnology*, vol. 3, no. 10, pp. 626–631, 2008.

[4] H. W. Yap, R. S. Lakes, and R. W. Carpick, "Mechanical instabilities of individual multiwalled carbon nanotubes under cyclic axial compression," *Nano Letters*, vol. 7, no. 5, pp. 1149–1154, 2007.

[5] H. W. Yap, R. S. Lakes, and R. W. Carpick, "Negative stiffness and enhanced damping of individual multiwalled carbon nanotubes," *Physical Review B*, vol. 77, no. 4, Article ID 045423, 2008.

[6] A. Sears and R. C. Batra, "Macroscopic properties of carbon nanotubes from molecular-mechanics simulations," *Physical Review B: Condensed Matter and Materials Physics*, vol. 69, no. 23, Article ID 235406, 2004.

[7] A. Sears and R. C. Batra, "Buckling of multiwalled carbon nanotubes under axial compression," *Physical Review B—Condensed Matter and Materials Physics*, vol. 73, no. 8, Article ID 085410, 2006.

[8] H. Xin, Q. Han, and X.-H. Yao, "Buckling and axially compressive properties of perfect and defective single-walled carbon nanotubes," *Carbon*, vol. 45, no. 13, pp. 2486–2495, 2007.

[9] X. Hao, H. Qiang, and Y. Xiaohu, "Buckling of defective single-walled and double-walled carbon nanotubes under axial compression by molecular dynamics simulation," *Composites Science and Technology*, vol. 68, no. 7-8, pp. 1809–1814, 2008.

[10] V. Parvaneh, M. Shariati, and A. M. Majd Sabeti, "Investigation of vacancy defects effects on the buckling behavior of SWCNTs via a structural mechanics approach," *European Journal of Mechanics, A/Solids*, vol. 28, no. 6, pp. 1072–1078, 2009.

[11] D. D. T. K. Kulathunga, K. K. Ang, and J. N. Reddy, "Molecular dynamics analysis on buckling of defective carbon nanotubes," *Journal of Physics Condensed Matter*, vol. 22, no. 34, Article ID 345301, 2010.

[12] R. H. Poelma, H. Sadeghian, S. Koh, and G. Q. Zhang, "Effects of single vacancy defect position on the stability of carbon nanotubes," *Microelectronics Reliability*, vol. 52, no. 7, pp. 1279–1284, 2012.

[13] M. Nishimura, Y. Takagi, and M. Arai, "Molecular dynamics study on buckling behavior of non-defective and defective triple-walled carbon nanotubes," *Journal of Solid Mechanics and Materials Engineering*, vol. 7, no. 3, pp. 403–416, 2013.

[14] Y. Kinoshita, M. Kawachi, T. Matsuura, and N. Ohno, "Axial buckling behavior of wavy carbon nanotubes: a molecular mechanics study," *Physica E*, vol. 54, pp. 308–312, 2013.

[15] H. Mori, S. Ogata, J. Li, S. Akita, and Y. Nakayama, "Energetics of plastic bending of carbon nanotubes," *Physical Review B*, vol. 74, no. 16, Article ID 165418, 2006.

[16] H. Mori, S. Ogata, J. Li, S. Akita, and Y. Nakayama, "Plastic bending and shape-memory effect of double-wall carbon nanotubes," *Physical Review B*, vol. 76, no. 16, Article ID 165405, 2007.

[17] S. J. Stuart, A. B. Tutein, and J. A. Harrison, "A reactive potential for hydrocarbons with intermolecular interactions," *Journal of Chemical Physics*, vol. 112, no. 14, pp. 6472–6486, 2000.

[18] E. Bitzek, P. Koskinen, F. Gähler, M. Moseler, and P. Gumbsch, "Structural relaxation made simple," *Physical Review Letters*, vol. 97, no. 17, Article ID 170201, 2006.

[19] T. Kitamura, Y. Umeno, and N. Tsuji, "Analytical evaluation of unstable deformation criterion of atomic structure and its application to nanostructure," *Computational Materials Science*, vol. 29, no. 4, pp. 499–510, 2004.

[20] T. Kitamura, Y. Umeno, and R. Fushino, "Instability criterion of inhomogeneous atomic system," *Materials Science and Engineering A*, vol. 379, no. 1-2, pp. 229–233, 2004.

[21] M. Kawachi, Y. Kinoshita, and N. Ohno, "Buckling behavior of wavy carbon nanotubes effects of the wavenumber and chirality," in *Proceedings of the Japan Society for Computational Methods in Engineering Symposium*, vol. 13, 2013.

[22] N. Ohno, D. Okumura, and T. Niikawa, "Long-wave buckling of elastic square honeycombs subject to in-plane biaxial compression," *International Journal of Mechanical Sciences*, vol. 46, no. 11, pp. 1697–1713, 2004.

[23] D. Okumura, A. Okada, and N. Ohno, "Buckling behavior of Kelvin open-cell foams under [0 0 1], [0 1 1] and [1 1 1] compressive loads," *International Journal of Solids and Structures*, vol. 45, no. 13, pp. 3807–3820, 2008.

[24] K. Kitamura, Y. Umeno, and Y. Kinoshita, "Evaluation of nonuniform strain in carbon nanotube with bend junction," *Journal of Solid Mechanics and Materials Engineering*, vol. 1, no. 11, pp. 1313–1321, 2007.